

*Article*

## Experimental Demonstration of Non-Hermitian Symmetry for DC-SC-FDM in UOWC Systems

Kidsanapong Puntsri<sup>1,\*</sup>, Ekkaphol Khansalee<sup>1</sup>, and Hanawa Masanori<sup>2</sup>

<sup>1</sup> Department of Electronics and Telecommunication, Faculty of Engineering, Rajamangala University of Technology Isan, Khon Kaen Campus, Khon Kaen, 40000, Thailand

<sup>2</sup> Department of Electrical and Electronic Engineering, University of Yamanashi, Japan

\*E-mail: kidsanapong.pu@rmuti.ac.th (Corresponding author)

**Abstract.** This study demonstrates the high spectrum efficiency of DC offset single-carrier frequency division multiplexing (DC-SC-FDM) for underwater optical wireless communications (UOWC). I and Q components were separately transmitted using dual lasers. As a result, the requirement of Hermitian symmetry is alleviated, and the computation time latency is reduced. The Gram–Schmidt orthogonalization procedure was adopted to address the I and Q orthogonality. The system comprises a 1024-point inverse fast Fourier transform (IFFT), a cyclic prefix of 32 samples, and a digital-to-analog converter (DAC) of 400 Msp/s, and laser diodes possess a wavelength of 553 nm with a power of 150 mW. The study includes real transmissions in a freshwater communication channel and reports experimental results. In addition, the bit error rate has been evaluated. The results show that at the forward error correction (FEC) limit, a communication distance of 10 m can be achieved. A peak-to-average power ratio reduction of 4.96 dB is reached.

**Keywords:** Underwater communication systems, optical wireless communication, orthogonal frequency division multiplexing, high spectrum efficiency.

ENGINEERING JOURNAL Volume 25 Issue 12

Received 5 October 2021

Accepted 19 December 2021

Published 30 December 2021

Online at <https://engj.org/>

DOI:10.4186/ej.2021.25.12.81

## 1. Introduction

Underwater communication systems based on visible light (VL) have been in demand for a decade. This new communication scheme aims to achieve low latency and high data rates [1] in underwater communication systems. In addition, high-definition video (HDV) is required for remotely controlled vehicles (ROVs) and autonomous underwater vehicles (AUVs), which require high data rates. However, traditional schemes, e.g., acoustic communication, are very difficult to achieve, owing to the limited transmission speed of 1.5 km/s of the acoustic signals, as reported in [2].

Underwater communication systems based on blue laser diodes (LDs) have been extensively investigated [3-5]. The transmission speed and capacity are better than those of traditional systems that use radio frequency (RF). In particular, when advanced modulation formats, e.g., orthogonal frequency division multiplexing (OFDM), are employed, the spectrum efficiency can be obtained, and the performance is superior to single-carrier (SC) communications, such as those applying pulse amplitude modulation (PAM) [6]. OFDM has several advantages over the SC. The main feature is that the intersymbol interference (ISI) is resolved by appending the cyclic prefix (CP), where the CP has to be longer than channel response taps. OFDM can insert pilot tones to lean the communication channel. This results in a simple implementation at the receiver part. However, a significant challenge is the high peak-to-average power ratio (PAPR), which makes the system prone to nonlinear distortion [7-8].

Single-carrier frequency division multiplexing (SC-FDM) exhibits a similar advantage to OFDM; however, the PAPR can be significantly reduced compared with OFDM [9]. In general, a DC offset (DC) is used to drive lasers; it can be known as DC-SC-FDM. Moreover, SC-FDM can be simply implemented in hardware components, requiring only an extra IFFT/FFT when compared with the conventional OFDM. Hermitian symmetry is employed when the SC-FDM is used in underwater communication systems, as detailed in [9]. Therefore, the spectrum efficiency has been reduced. In recent times, there have been studies on schemes free of Hermitian symmetry, where the spectrum efficiency is

improved. In particular, Azim et al. [10] showed that the Hermitian symmetry free for optical SC-FDM in visible light communication (VLC) can be removed by sequentially sending I and Q components: first the real component and then the imaginary component. In this case, the processing time increased. As a result, the spectrum efficiency is the same as that of the traditional one. In [11-12], non-orthogonal multiple access (NOMA) for a VLC system without Hermitian symmetry was proposed. The scheme is similar to that of [9], and the real and imaginary components are sequentially transmitted. As a result, the system suffers from low-spectrum efficiency.

In this study, a new high-spectrum-efficiency transmission scheme without Hermitian symmetry and with a low PAPR modulation format is proposed for underwater communication systems. Moreover, it is known as dual laser diode (LD) DC-SC-FDM, where the I and Q components are separately transmitted using dual LDs. This is a novel investigation. In addition, I and Q orthogonal issues are compensated based on a Gram-Schmidt orthogonalization procedure (GSOP) [13]. The investigation was performed in real-world transmissions in a fresh underwater channel and analyzed offline using MATLAB®.

At the transmitter side, the DC-SC-FDM symbol is pre-generated offline and saved into read-only memory (ROM) inside the field-programmable gate array (FPGA), while the received DC-SC-FDM symbol is saved in the oscilloscope and analyzed using MATLAB®. Lasers of wavelength 553 nm and power 150 mW were used. The experimental results show that the PAPR for the DC-SC-FDM is only 6.44 dB, and a communication distance of 10 m can be achieved at the forward error control (FEC) limit of  $2.8 \times 10^{-3}$ .

## 2. Description of DCO-SC-FDM for UIWC

In this section, SC-FDM for underwater optical wireless communication systems are presented and described, where non-Hermitian symmetry and high spectrum efficiency are achieved. Figure 1 illustrates the system.

At the transmitter part, the bit stream is fed into a

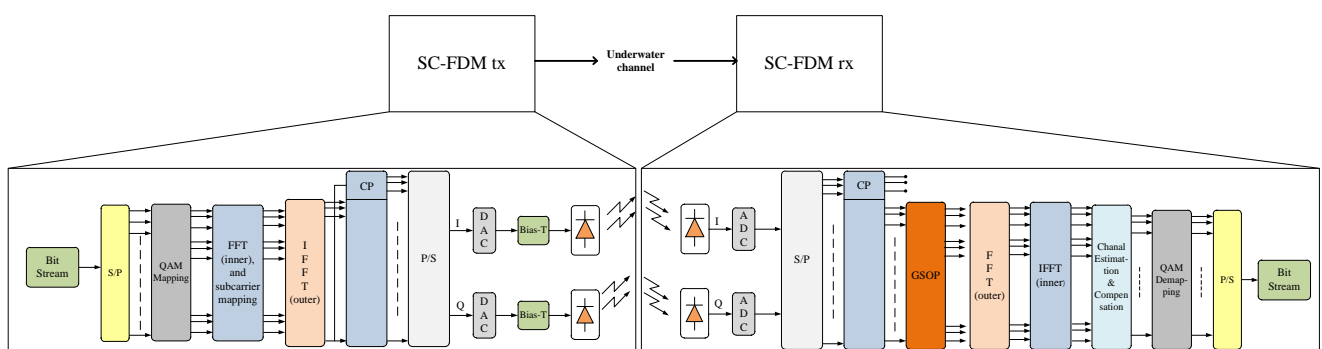


Fig. 1. DCO-SC-FDM for underwater communication systems using duo lasers.

QAM mapper, where a group of bits is mapped into  $M$ -ary QAM symbol  $s$ , where  $M$  is the constellation size. The QAM symbols are converted to the frequency domain using fast Fourier transform (FFT). Then, subcarrier mapping based on inverse FFT (IFFT) is implemented, where interleaved FDM subcarrier mapping is used. It has exhibited the lowest PAPR [8]. In this study, an IFFT size of  $N=1024$  is assumed. Therefore, to implement all the subcarriers, we have considered the inner FFT size to be  $N/2$ . Next, the output values of all the inner FFTs are converted to the time domain using the outer IFFT, and the CP appears as follows. The subcarrier mapping is expressed as

$$\mathbf{X} = [0, s_0, 0, s_1, \dots, 0, s_{N/2-1}, 0, s_{N/2-1}^*, 0, s_{N/2-2}^*, \dots, 0, s_0^*], \quad (1)$$

where  $\mathbf{X}$  is the vector input for outer IFFT. After considering IFFT, the output is denoted by  $\mathbf{x} = \text{ifft}(\mathbf{X})$ .  $\mathbf{x}$  is a complex number, which is included in phase, denoted by  $I$ , and the quadrature part is denoted by  $Q$ . Next, the CP is added to the head to prevent ISI. In this study,  $I$  and  $Q$  components are separately transmitted using dual LDs as signals denoted by  $x_I(n)$  and  $x_Q(n)$ , respectively.

At the receiver part, as illustrated on the right-hand side of Fig. 1, the received light signal is converted to an electrical signal using an avalanche photodiode (APD). The received electrical signals of the  $I$  and  $Q$  components are  $y_I(n)$  and  $y_Q(n)$ , respectively, which are obtained using

$$y_I(n) = x_I(n) * h_I(n) + z_I(n), \quad (2)$$

and

$$y_Q(n) = x_Q(n) * h_Q(n) + z_Q(n), \quad (3)$$

where  $*$  denotes a linear convolution operator. For the  $I$  and  $Q$  components,  $h_I(n)$  and  $h_Q(n)$  denote channel responses, and  $z_I(n)$  and  $z_Q(n)$  are the additive white Gaussian noise (AWGN) with zero mean and variance of  $\sigma_z$ , respectively. Next, GSOP is followed. Let us define the pairs of GSOP sets for  $I$ , denoted as  $y_I^o(n)$ , and  $Q$  component as  $y_Q^o(n)$ , which are obtained using

$$y_I^o(n) = y_I / \sqrt{p_I}. \quad (4)$$

Here,  $p_I = E \{y_I^2(n)\}$ , where  $E \{ \cdot \}$  stands for average operator and

$$y_Q^o(n) = y_Q / \sqrt{p_Q}, \quad (5)$$

where  $p_Q = E \{y_Q^2(n)\}$  and

$$y_Q^o(n) = y_Q(n) - E \{y_I(n) \cdot y_Q(n)\} / p_I. \quad (6)$$

The received signals are combined:  $y^o(n) = y_I^o(n) + jy_Q^o(n)$ . Applying FFT, we obtain

$$\begin{aligned} Y^o(k) &= \text{FFT} \{y^o(n)\} \\ &= \text{FFT} \{y_I^o(n)\} + j \text{FFT} \{y_Q^o(n)\}, \quad (7) \\ &= X_I^o(k)H_I^o(k) + j X_Q^o(k)H_Q^o(k) + Z^o(k) \end{aligned}$$

where  $Y^o$  is the received signal after applying the GSOP, and  $Z^o(k) = Z_I^o(k) + jZ_Q^o(k)$  is the AWGN noise.

$H_I^o(k)$  and  $H_Q^o(k)$  are channel responses, which are considered to be the same because they are installed very close to each other. Therefore,  $H_I^o(k) = H_Q^o(k) = H^o(k)$ ; this is a real number [10]. Eq. (7) can be rewritten as

$$Y^o(k) = H^o(k) X_I^o(k) + jX_Q^o(k) + Z^o(k). \quad (8)$$

All of these equations are explained in the frequency domain.

### 3. Channel Estimation and Compensation

In this study, for channel estimation, the pilot-aided method was used to learn channel information. As a result, the estimated channel responses, denoted by  $\tilde{H}(k)$ , can be extracted by dividing the received signal based on known pilots, which is defined by [11].

$$\begin{aligned} \tilde{H}(k) &= \frac{Y_p(k) \cdot Xp^*(k)}{|Xp(k)|^2} \\ &= \frac{Xp(k) \cdot H(k) \cdot Xp^*(k)}{|Xp(k)|^2} + \frac{Z(k)}{|Xp(k)|^2}, \quad (9) \\ &= H(k) + \frac{Z(k)}{|Xp(k)|^2} \end{aligned}$$

where  $Y_p(k)$  is the received pilot signal and  $Xp(k)$  is the transmitted known pilot signal. Next, to remove the channel impairment of the received signal by considering the conjugate and multiplying it back to the received signal, which is explained by

$$\tilde{Y}(k) = \frac{Y^o(k)}{\tilde{H}(k)}. \quad (10)$$

$\tilde{Y}(k)$  where is the estimated symbol. Therefore, based on Eq. (10), if  $\tilde{H}(k) = H(k)$  is assumed, the estimated symbols at the received signal are given by

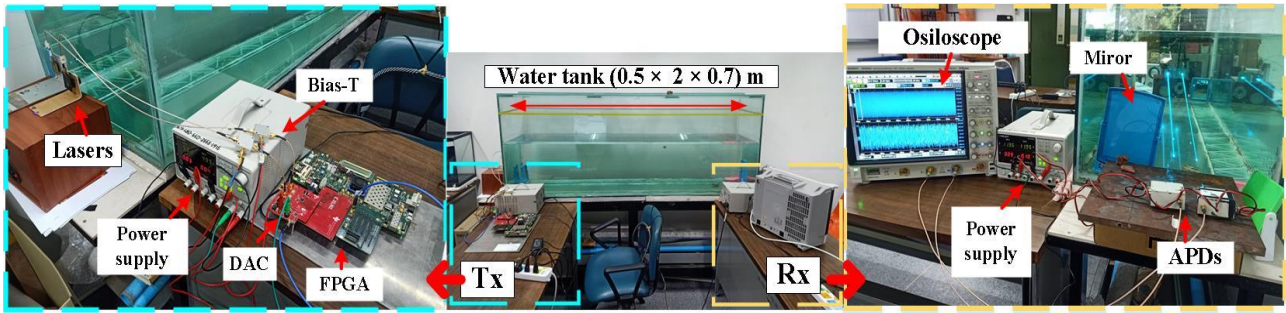


Fig. 2. Experimental setup of UOWC SC-FDM communication systems.

$$\begin{aligned} \tilde{Y}(k) &= H(k) X_I(k) + jX_Q(k) + Z(k) \frac{1}{\tilde{H}(k)} \\ &= X_I(k) + jX_Q(k) + \frac{Z(k)}{\tilde{H}(k)} \end{aligned} \quad (11)$$

#### 4. PAPR Description

The PAPR is calculated as

$$PAPR = \frac{\max |s_n|^2}{E |s_n|^2}, \quad (12)$$

where  $s_n$  denotes the arbitrary waveforms of OFDM and SC-FDM signals in the time domain.  $|\cdot|$  is the absolute value, and  $E\{\cdot\}$  denotes the expectation calculation. Moreover, a PAPR is measured based on the complementary cumulative distribution function (CCDF), which is given by

$$P_c = \Pr \{PAPR > \lambda\}. \quad (13)$$

$P_c$  is the probability that PAPR exceeds a particular value of  $\lambda$ . In addition, the PAPR performance comparison is presented in [9]. The results showed that SC-FDM exhibited the best performance in terms of PAPR reduction.

#### 5. Experimental Setup

This section details the proposed I and Q components separately transmitted using dual LDs for the SC-FDM. The SC-FDM transmitter (Tx) and receiver (Rx) are shown in Fig. 1, while the experimental setup is shown in Fig. 2. At the transmitter part, SC-FDM symbols are pre-generated in a digital format using MATLAB@. The first two symbols are used as pilot symbols to learn the underwater channel and phase rotation, as shown in Eqs. (9) and (10). The digital signal is converted to an analog signal at an update rate of 400 Msps based on a dual data rate. Dual blue-green light

lasers with a power of 150 mW were used. In addition, an outer IFFT size of 1024 with 32 samples of CP was employed, and 8-QAM and 16-QAM were considered to be used in each subcarrier.

As the LDs required only zero and positive, the analog time domain SC-FDM signal must be offset by Bias-Ts (ZFBT-4R2GW+). The optimum bias point, to avoid the nonlinearity region, as shown in [8, 12, 14], is 5.2 V. The received light was converted to an electrical signal by APD (Hamamatsu CD5658) with a bandwidth of 1 GHz. The received electrical signals of I and Q were saved into an oscilloscope (DSOS604A) and analyzed using MATLAB@. The fresh water tank of 0.5 m  $\times$  2 m  $\times$  0.7 m was used. In addition, the bit error rate (BER) is used as a system performance metric, where the communication distance is considered. In addition, the distance was extended by mirrors on both sides of the tank.

#### 6. Experimental Results

In this section, the experimental results of SC-FDM with I and Q separately transmitted using dual lasers for UOWC are presented. As shown in Fig. 3, the BER of 8-QAM against distances is studied, and the SC-FDM and OFDM are compared. OFDM has the same setup as SC-FDM. A communication distance of 8 m can be achieved. In addition, the BER of the SC-FDM is slightly the same

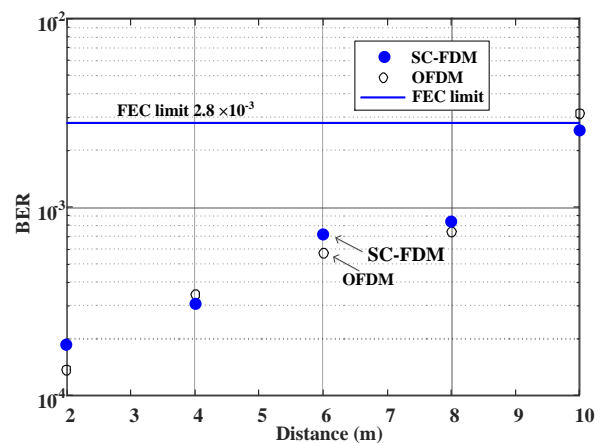


Fig. 3. BER performance comparison of SC-FDM and OFDM for 8-QAM.

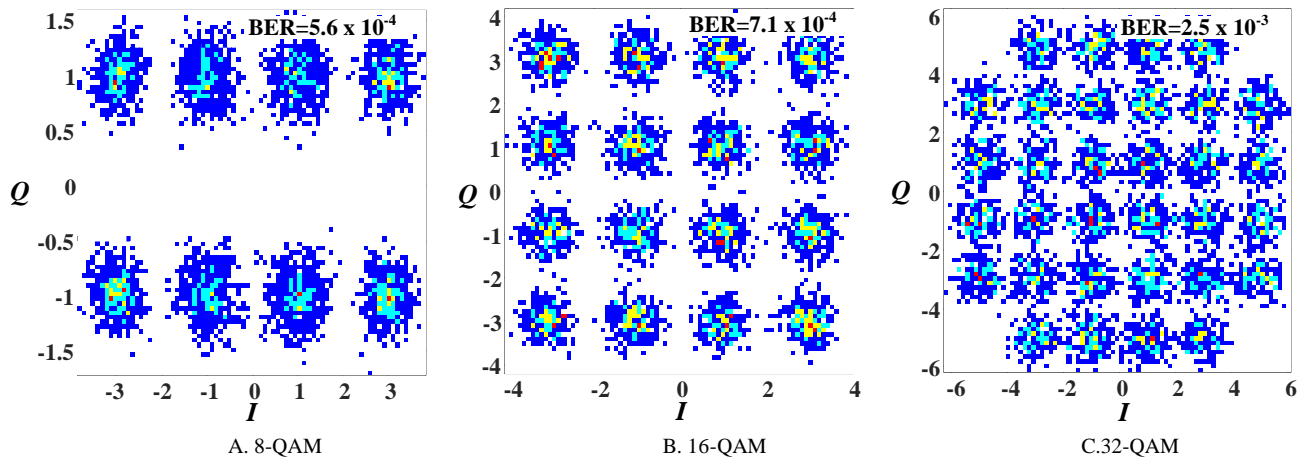


Fig. 4. Constellation plot at 6 m for: A. 8-QAM, B. 16-QAM, and C. 32-QAM for SC-FDM.

as that of the conventional OFDM. This confirms that there is no general loss. Next, the QAM orders of 8-QAM, 16-QAM, and 32-QAM at a distance of 6 m are studied. The BERs of  $5.6 \times 10^{-4}$ ,  $7.1 \times 10^{-4}$ , and  $2.5 \times 10^{-3}$  are achieved. The constellations are shown in Fig. 4. 8-QAM is clear, and it gets worse for 16-QAM and 32-QAM. However, 32-QAM can be achieved, where the BER is below the FEC limit. Moreover, the curve shows that the BER increases when the distance increases beyond the FEC limit.

Finally, the PAPR results of OFDM and SC-FDM at the Rx are 11.13 and 6.44 dB, respectively. This signifies a considerable improvement in nonlinearity impairment owing to LDs. Although the SC-FDM comprises more operations of implementation in hardware than the conventional OFDM, it is implementable with regard to hardware.

## 7. Conclusion

This study proposed dual lasers to separately transmit I and Q components for DC-SC-FDM underwater optical communication systems. As a result, Hermitian symmetry can be free, and the spectrum efficiency is improved, when compared with conventional schemes. This is a new study. The system performance was experimentally demonstrated using a real fresh underwater communication channel. The OFDM symbol was pre-generated using MATLAB@ and saved into the FPGA. A DAC speed of 400 Msps was considered. Blue–green-light lasers with a power of 150 mW were employed. The number of subcarriers was 1024, each modulated by 8-QAM, and 32 CP samples were obtained. The results show that a communication distance of 10 m can be achieved at the FEC limit. In addition, a PAPR reduction of 4.96 dB was achieved compared with the OFDM.

## Acknowledgment

This research project has been supported by the Rajamangala University of Technology Isan. Contract No. ENG14/64. We would like to thank our department and anonymous reviewers for their useful comments.

## References

- [1] H. Kaushal and G. Kaddoum, "Underwater optical wireless communication," *IEEE Access*, vol. 4, pp. 1518–1547, 2016.
- [2] Li-L. Hung and Y-J. Luo, "Protocol to exploit waiting resources for UASNs," *Sensors*, vol. 16, no. 3, pp. 333–338, 2013.
- [3] S. Arnon, "Underwater optical wireless communication network," *J. Opt. Eng.*, vol. 49, no. 1, 2010.
- [4] X. Yi, Z. Li, and Z. Liu, "Underwater optical communication performance for laser beam propagation through weak oceanic turbulence," *Appl. Opt.*, vol. 54, no. 6, pp. 1273–1278, 2015.
- [5] K. Nakamura, I. Mizukoshi, and M. Hanawa, "Optical wireless transmission of 405 nm, 1.45 Gbit/s optical IM/DD-OFDM signals through a 4.8 m underwater channel," *Opt. Express*, vol. 23, pp. 1558–1566, 2015.
- [6] K. Puntsri and E. Khansalee, "Experimental comparison of OFDM SC-FDM and PAM for low speed optical wireless communication systems," in *2019 7th International Electrical Engineering Congress (iEECON)*, Hua Hin, Thailand, 2019, pp. 1–4.
- [7] J. Armstrong, "OFDM for optical communications," *J. Lightwave Technol.*, vol. 27, no. 3, pp. 189–204, 2009.
- [8] P. Tasao, K. Puntsri, and E. Khansalee, "Peak to average power ratio analysis of single carrier FDMA plus soft-clipping for PON systems," in *15th International Conference on Electrical Engineering/Electronics, Computer, Telecommunications*

- and *Information Technology (ECTI-CON)*, 2018, pp. 449-452.
- [9] K. Puntsri, "Experimental demonstration of high spectral efficiency SC-FDMA with soft clipping for optical wireless communication systems," *IET Optoelectron.*, vol. 12, no. 2, pp. 80–85, 2018.
- [10] A. W. Azim, Y. L. Guennec, and G. Maury, "Hermitian symmetry free optical-single-carrier frequency division multiple access for visible light communication," *Opt. Commun.*, vol. 415, pp. 177–185, 2018.
- [11] A. Adnan, Y. Liu, C. Chow, and C. Yeh, "Demonstration of non-Hermitian symmetry (NHS) IFFT/FFT size efficient OFDM non-orthogonal multiple access (NOMA) for visible light communication," *IEEE Photonics J.*, vol. 12, no. 3, pp. 1–5, 2020.
- [12] F. Barrami, Y. Le Guennec, E. Novakov, J. Duchamp, and P. Busson, "A novel FFT/IFFT size efficient technique to generate real time optical OFDM signals compatible with IM/DD systems," in *2013 European Microwave Conference*, pp. 1247-1250.
- [13] I. Fatadin, S. J. Savory, and D. Ives, "Compensation of quadrature imbalance in an optical QPSK coherent receiver," *IEEE Photonics Technol. Lett.*, vol. 20, no. 20, pp. 1733–1735, 2008.
- [14] K. Puntsri, E. Khansalee, and P. Suttisopapan, "Diversity based on oversampling technique for PAM-4 in optical wireless communication systems," *Eng. J.*, vol. 24, no. 4, pp. 133-141, 2020.



**Kidsanapong Puntsri** received the bachelor of engineering degree in telecommunication engineering from the Mahanakorn University of Technology (MUT), Thailand, in 2002, and master of engineering degree in telecommunication engineering from King Mongkut's Institute of Technology Ladkrabang (KMUTL), Thailand, in 2004. In 2014, he obtained Dr.-Ing in optical communication from Paderborn University, Germany. At present, he is an assistant professor at the Department of Electronics and Telecommunication Engineering, Rajamangala University of Technology Isan, Khon Kaen Campus, Thailand. His main research interests include multi-carrier communication in optical and wireless systems and realization of communication systems based on field-programmable gate array (FPGA). He has published more than 40 contribution papers in IEEE and is a senior IEEE member.



**Ekkaphol Khansalee** received the bachelor of engineering degree in electronics and telecommunication engineering from Rajamangala University of Technology Isan, Khon Kaen Campus (RMUTI KKC), Thailand, in 2008, and the M.Sc. degree in communication engineering from King Mongkut's University of Technology North Bangkok (KMUTNB), Thailand, in 2013. At the present, he is a lecturer at the Department of Electronics and Telecommunication Engineering, RMUTI KKC, Thailand. His main research interests include radio frequency and microwave circuit design in wireless power transfer systems, radio frequency energy harvesting systems, and optical wireless communication systems. He has published 12 contribution papers in IEEE.



**Hanawa Masanori** received B.E., M.E., and Ph.D. degrees all from Saitama University, Japan, in 1990, 1992, and 1995, respectively. In 1995, he joined the University of Yamanashi, Japan, as a research associate. Currently he has served as a professor, a director for the center of higher education, a president assistant, and a director of the department of Electrical and Electronics Engineering at the university. His research interests include optical fiber communications, underwater optical wireless communications, biomedical signal processing, and applications of machine learning. He is a member of IEEE, IEICE, OSA, JSET. He was received as the Distinguished Educational Practitioner Award in the IEICE in 2018.